Iraqi Geological Journal

Journal homepage: https://www.igj-iraq.org

Assessment of Erosion Risk and Sustainable Mitigation Strategies: A Case Study of Agoudal Watershed (High-Atlas, Morocco)

Youssef Ouadjane[1], Brahim Benzougagh[2,3*], Ayad M. Al-Quraishi[4], Youssef Bammou[5], Hanane Najem[6], Laila Nassiri[1], and Jamal Ibijbijen[1]

1 Environment and Valuation of Microbial and Plant Resources Team (EVRMV), Biology Department, Faculty of Sciences, Moulay Ismail University, Meknes-City, Morocco
2 Department of Geomorphology and Geomatics, Scientific Institute, Mohammed-V University in Rabat, Avenue Ibn Batouta, Rabat, Morocco
3 Laboratory of Geoengineering and Environment, Cartography and Tectonophysics team (CaTec), Department of Geology, Faculty of Sciences, Moulay Ismail University, Meknes, Morocco
4 Petroleum and Mining Engineering Department, Tishk International University, Erbil, Iraq
5 Laboratory of Geo-Resources, Geo-Environment and Civil Engineering (L3G), Department of Geology, Faculty of Science and Technology, Cadi Ayad University, Marrakesh, Morocco
6 Laboratory of A lied and Marine Geosciences, Geotechnics and Geohazards (LR3G), Department of Geology, Faculty of Sciences, Abdelamlek Essaâdi University, Tetouan, Morocco
* **Correspondance**: brahim.benzougagh@is.um5.ac.ma and benzougaghbrahim@gmail.com

Received:
12 November 2024
Accepted:
31 Juhy 2025
Published:
30 November 2025

Abstract

The Agoudal watershed, situated in the region of Draa-Tafilalet, the province of Midelt in southeastern Morocco, is the upstream part of the Imilchil valley. These delicate habitats, which span the central great Atlas altitudinal range from 2400 to more than 3150 m, are under great risk of erosion because of their poorly protected and unarable soils. Climate change, biological issues, and anthropogenic activities have all contributed to the region's extensive deterioration. This study uses the RUSLE approach in conjunction with GIS and remote sensing to evaluate erosive processes in the Agoudal sub-watershed and identify priority susceptible areas. An inventory of the study area is conducted to target hot spot areas, establishing a development map as the basis for implementing sustainable mechanical and biological mitigation measures. The results demonstrate reliable simulation of water erosion dynamics by the RUSLE model. Almost the entire basin faces severe soil degradation, with approximately 66% falling into specific degradation classes of 50 to 400 tons per hectare per year, and 18.9% displaying low to medium rates ranging from 7.4 to 32.17 tons per hectare per year. Only 1.4% of the watershed experiences degradation rates below 7.4 tons per hectare per year. The average soil loss rate is 255 tons per hectare per year, with a standard deviation of around 285 tons per hectare per year, reflecting the environment's heterogeneity. These figures attest to the high erosion risks in the region, compounded by recurrent floods, endangering food agriculture. Urgent mitigation intervention is necessary to address this alarming situation and protect the area's agricultural productivity.

Keywords: Water Erosion; Soil Loss; Geographical Information System; Remote Sensing; Management Model; Agoudal watershed; Morocco

1. Introduction

Soil deterioration and erosion are major subjects in earth sciences that have been investigated from a variety of perspectives and are of great interest to a wide range of academics. These include understanding sediment transport, water fluxes, and extreme storm events at catchment scales (Keesstra

et al., 2018; Lizaga et al., 2019; Benzougagh et al., 2022), the production of sustainable agriculture (Tarolli et al., 2019), examining the effects of soil erosion on biogeochemical cycling (Quinton et al., 2010; Lugato et al., 2016; Lal, 2019; Tan et al., 2020), and climate change (Borrelli et al., 2018; Ricci et al., 2018; Panagos and Katsoyiannis, 2019; Batista et al., 2019).

Worldwide, land degradation and, particularly, anthropogenic factors, as well as climate change, are among the most pressing challenges. It affects approximately 25% of Earth's surface and threatens the livelihoods of more than 900 million people in approximately 100 countries (Benbrahim et al., 2004; Brahim et al., 2020).

Morocco actively suffers from this problem, affecting approximately 43% of its territory (FAO, 1996). The loss of topsoil is estimated at approximately 22,000 ha/year (Croitoru and Sarraf 2017) and more than 12,000,000 hectares of which 1/3 of the arable land is threatened with degradation by erosion (Benbrahim et al., 2004). Of the 23 million hectares in mountainous areas, 75% are affected by erosion, one-third of which is very critical (Badraoui and Hajji, 2001; Brahim et al., 2020; Benzougagh et al., 2023). These landscapes are degraded in numerous ways, primarily due to natural reasons, mostly related to climate change and human activity, such as overgrazing, deforestation, and urbanization. Degradation on cultivated land impacts around 160,000 hectares of irrigated land through salinization and 5.5 million hectares of rainfed regions (due to erosion); these losses are estimated to be 1.7 billion Dollar. This issue also impacts rangelands due to overexploitation (30.2 million ha/year), desertification (103,000 ha/year), and clearance (65,000 ha/year) (Croitoru et al., 2017).

The study area is a typical case for the phenomenon of water erosion, where the soil suffers from a lack of vegetation and undergoes an aggressive climate with stormy rainfall as very localized in time and space (Brahim et al., 2020). This causes soil loss beyond pedogenesis to compensate for these losses. Reduced crop yields, a decrease in the surface area of agricultural soils, which are already not very arable, and an accelerated rate of silting of reservoirs and downstream hydraulic infrastructure are the results of this deterioration of biodiversity. Despite the efforts made by the local communities to fight against this plague, through essentially mechanical corrections in the absence of scientific studies, the results are very limited and transitory. Numerous researchers worldwide, including those in Morocco, have employed this method to evaluate and map the danger of water erosion (Anys et al., 1992, 1994; Bennmoussa et al., 1993; Brahim et al., 2020; Elalaoui et al., 2015; El Garouani et al., 2003, 2005, 2008; Issa et al., 2016; Merkhi et al., 2015; Ouallali et al., 2016).

The present study aims to propose a more resilient and sustainable erosion control model in the Assif Melloul watershed by first quantifying the erosive processes using the RUSLE model coupled with Remote Sensing (RS) and GIS, as an essential step in determining and spatializing "hot spot" areas. Then, we propose a map of targeted and sustainable anti-erosion management upstream of this watershed, which proposes a combination of mechanical work with biological anti-erosion actions integrating indigenous shrubs with potential ecological resilience and multiple uses.

The primary objectives of this study are threefold: (i) to assess erosive processes within the Agoudal sub-watershed, situated upstream of the main study area, by applying the Revised Universal Soil Loss Equation (RUSLE) in combination with Remote Sensing (RS) and Geographic Information Systems (GIS) for the identification of priority erosion-prone zones; (ii) to conduct a detailed inventory of the study area in order to delineate and characterize hot spot regions; and (iii) to develop a targeted development map that will provide a scientific basis for the implementation of sustainable mechanical and biological erosion-control measures, with particular emphasis on the utilization of two indigenous shrub species, Berberis hispanica Boiss. & Reut and Ribes uva-crispa L. In our opinion, such an approach could constitute a sustainable and resilient model of watershed management in mountainous areas that is adaptable, transferable, and applicable to similar situations.

2. Materials and Methods

2.1. Materials

2.1.1. Geology of the area

The Agoudal watershed is a subwatershed of Oued Ahnsal, whose altitudinal range goes from 2400 to more than 3150 m, is located about 20 km southeast of the center of Imilchil, upstream of the Assif Melloul watershed, whose waters flow into the Oued Ahnsal and constitute a hydrographic network of the Moroccan Central High Atlas, which leads to the Bin El Widane reservoir (Fig.1). It covers an area of about 6240 ha, and is framed by two quadrilaterals of coordinates: (X1: 471638, Y1: 173013) and (X2: 479859, Y2: 180436). It is administratively under the territorial community of Bouzmou, the circle of Imilchil, in the region of Draa-Tafilalet, Midelt province. This watershed is characterized by its very rugged terrain, harsh climatic conditions, and the degradation of its vegetation cover under the effects of climate change and zoo anthropic action, and provides a typical case for the phenomenon of water erosion (Ouadjane et al., 2021).

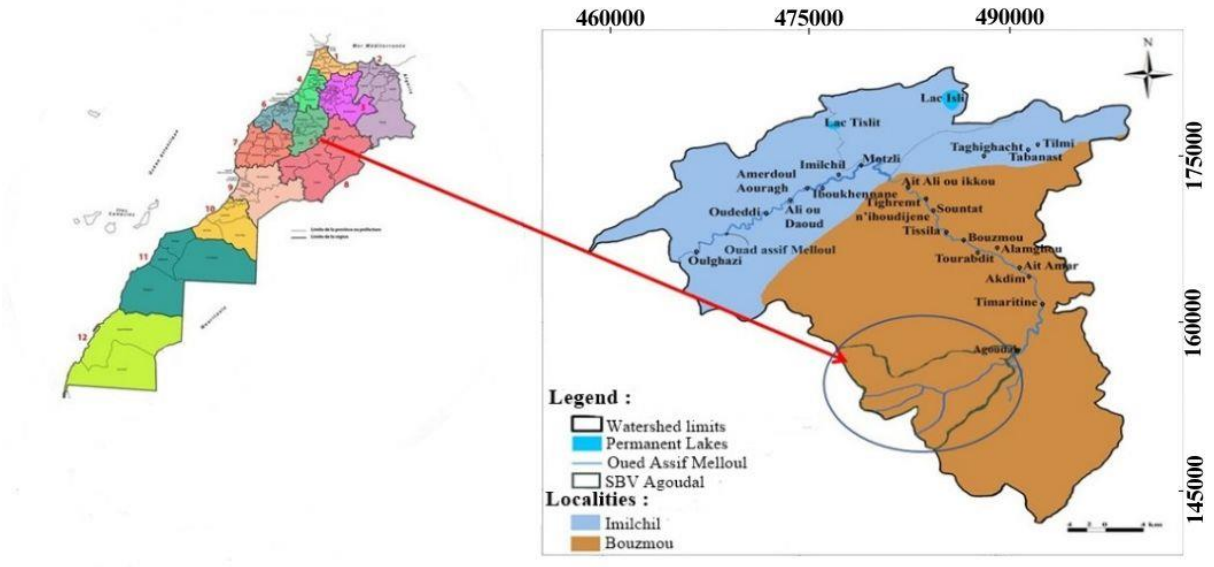


Fig.1. Geographical location of the Agoudal watershed

According to the geology shown in Fig.2, massive synclines that alternate laterally with small anticlinal structures (ridges) with amplitudes of up to hundreds of meters encircled the Agoudal watershed in both its northern and eastern regions (Michard et al., 2011; Ibouh and Chafiki 2017). It is situated between the Toumliline and Ikerzi Ridges. The latter are mostly oriented east-west orientated and are cored by Jurassic alkaline gabbro, Liassic limestone, and Triassic basalts. As with the whole High Atlas range, these formations are primarily dominated by Jurassic marly-limestone strata (Fig. 2), which cover nearly the entire surface of BV Assif Melloul (Laville et al., 1977). They expose a sedimentary series of Liassic to Bajocian-Bathonian marine limestone, with widespread red beds in the Bathonian strata and tholeiitic basalts (Choubert and Faure-Muret 1960; Jenny et al., 1981). The second Jurassic series was composed of carbonate and shale deposits capped by terrigenous red beds (Charrière and Haddoumi, 2016). The impermeable Toarcian-Aalenian series, where the valleys are located, shares the surface with the limestone, limestone-marl, and marl series from the Toarcian to Bajocian. The Jurassic ended with a series of mostly sandstone, continental, and red facies (Upper Jurassic), passing to the Lower Cretaceous. Because of many erosion processes, only the remnants of the Upper

Paleocene-Eocene subaerial deposits have survived on the fractured ridges (Charrière et al., 2009; Michard et al., 2011).

Terrigenous red beds constitute the top Cretaceous layers, whereas Cenomanian-Turonian limestone comprises Cretaceous strata (Amrhar 1995; Froitzheim et al. 1988). In general, the geological Formations of Assif Melloul have compact, hard, and encrusted lithological features. Those exposed to strong alterations have already reached an advanced stage due to the aggressive climatic conditions associated with the amplifying effects of climate change and anthropic action that have led to land degradation and soil loss by water erosion (Boudhar et al., 2007).

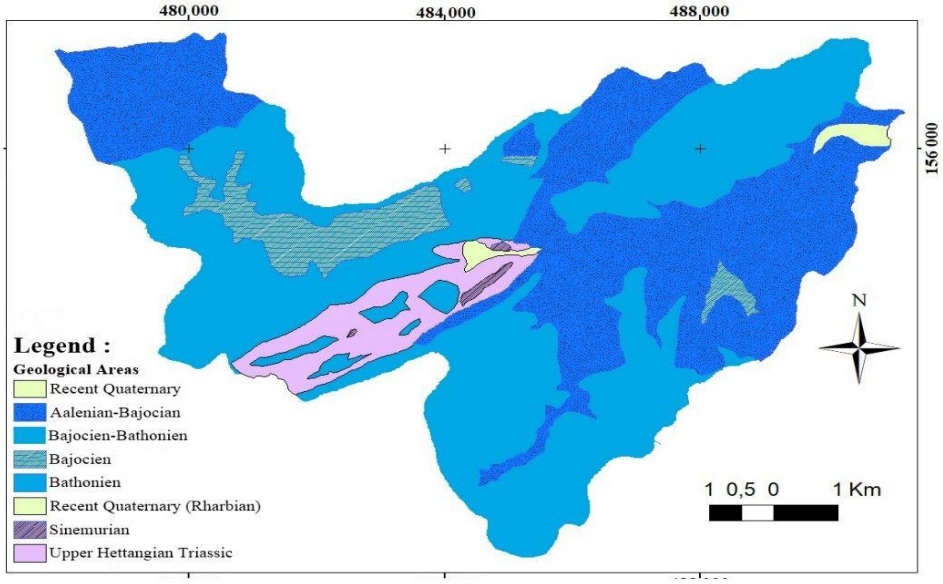


Fig. 2. Geological map of the Agoudal watershed

As shown in Fig. 3, the study area has a fine structure with granulometry characterized by a concentration of silt and fine sand eroded from the bedrock slopes (Ouadjane et al., 2021).

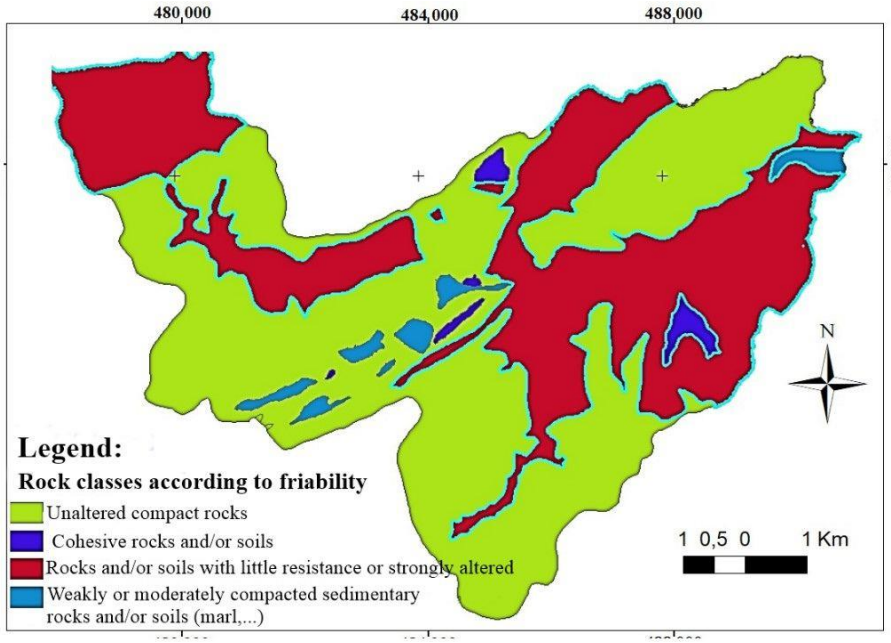


Fig. 3. Map of friability classes of rocks in the Agoudal watershed

2.1.2. Climate context

The climate in the study area is characterized by a semi-arid bioclimate with cold to very cold winters, with snowfall and an average rainfall of 317 mm at Imilchil. This is characterized by significant inter-annual variability oscillating between dry and wet years. They fluctuate from 49.5 mm/year during the 1982-1983 seasons to 661 mm/yr during the 1995-1996 seasons. The absolute minimum temperature of the coldest month reaches -18 °C with an average of the minima of as -5.1°C and the average of the maxima of 32.4°C (Mrabet et al., 2020).

The near absence of perennial vegetation with trees or shrubs means that the residues left on the ground do not allow for the restoration of organic matter, which can promote this soil structure, with the exception of cultivated plots. Intensive deforestation linked to grazing activities and overexploitation of wood by the population (cooking and heating), combined with climatic hazards, further aggravated the phenomena of erosion and massive soil loss.

2.2. Methods

In order to accomplish the goal of mapping the Agoudal watershed's soil susceptibility to water erosion, we used an approach was used which based on (Renard et al., 1991) Revised Universal Soil Loss Equation (RUSLE). For both natural and agricultural lands, the RUSLE model has been widely used to assess the risk of soil erosion and predict the yearly rate of soil loss. Data from gauge stations, remote sensing, and other sources were used in this study. Fig. 4 depicts the workflow created to fulfill the goal of this study. The sub-sections offer a thorough explanation of this process. One of the most experimental studies that has used mathematical models to examine the yearly rates of water erosion is the universal equation of soil loss (RUSLE). The (RUSLE) model is a worldwide hybrid adaptable model that offers unbiased and trustworthy results for evaluating the geographical distribution of soil erosion when combined with remote sensing (RS) and geographic information systems (GIS). An erosion control map was created based on the findings of the hotspot regions and soil loss quantification with the (help of the RUSLE.

In both cases, the (RUSLE) model offers the best framework for evaluating the rate of soil loss and its contributing components. In particular, (RUSLE) views topography (LS), cover management (C), rainfall (R), soil erodibility (K), and support practices (P) are significant determinants of soil loss rate. The following mathematical equation (Eq. 1) represents (RUSLE), a:

$$A = R \times K \times C \times SL \times P \quad (1)$$

Where**:**

A: Soil loss rate (t/ha/yr)

R: Rainfall erosivity (MJ.mm/ ha.h.y)

K: Soil erodibility (t.h/ha. MJ.mm)

LS: Topographic factor (L in m, S in %)

C: Vegetation cover factor

P: Cultivation practice factor.

Each factor represents a numerical estimate of an element that influences the degree of soil erosion in a particular area.

2.3. Description of Erosion Factors

2.3.1. Factor LS: Topography

Topography plays a crucial role in determining the length and inclination of the slopes, as well as the many stages of the erosion process, particularly the sediment transport phase. In these

high-mountain regions, topography plays a major role in erosion. The higher their levels, the more active the erosion of slopes and the higher the runoff, which increases the likelihood of flooding.

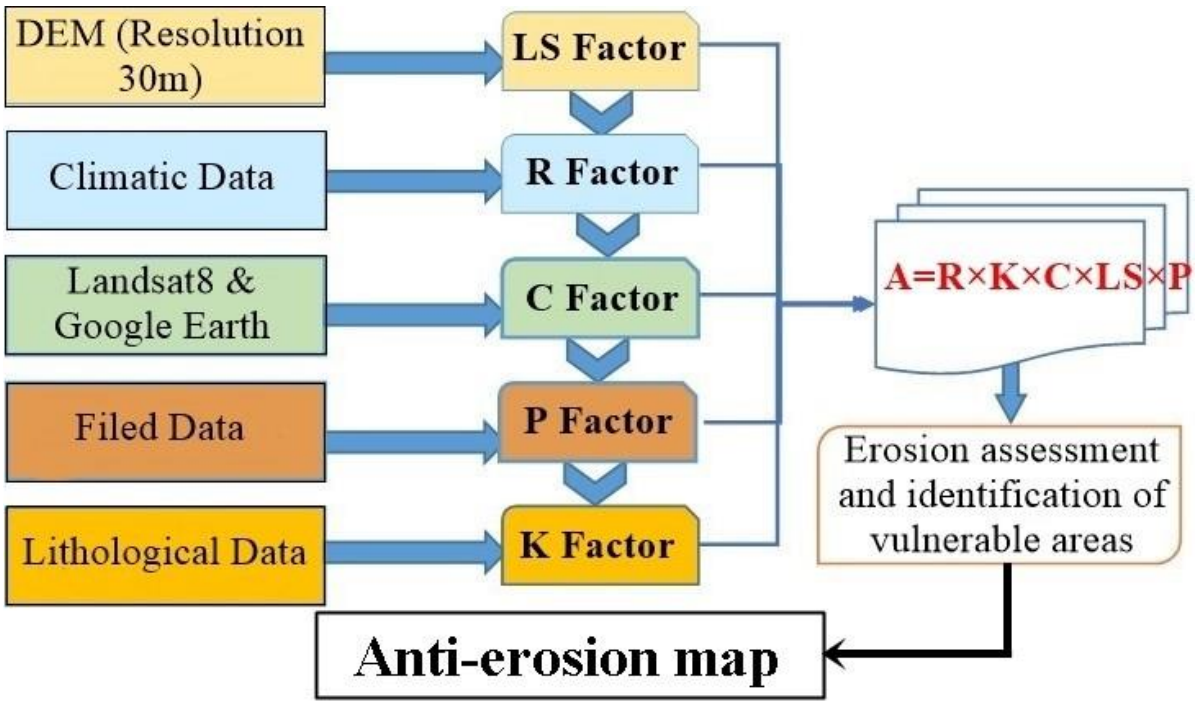


Fig. 4. Flowchart of RUSLE model work methodology

A topographic study of the study area was conducted based on the most accurate data available, including topographic maps at a scale of 1/50,000 (Sheets: Outerbat, Imilchil Aghbalou N'Kerdous and Aghendou N'Ouerz), which were geo-referenced and digitized. Based on the digital terrain model (DTM) of 30 m resolution, downloaded from the website (https://earthexplorer.usgs.gov), the LS factor was evaluated by applying Equation (Eq. 2), developed by Mitasova et al. (1996):

$$LS = (L|22.13)m \times (65.41Sin2(S) + 4.56Sin(S) + 0.065) \quad (2)$$

Where:

L: slope length (m); S: Slope inclination (%).

m: constant, which is equal to 0.5, for slopes greater than 5%. 0.4 for slopes between 3.5 and 5%, respectively. 0.3 for slopes ranging from 1 to 3.5%. 0.2 for slopes of less than 1%.

For the most common slopes (0.1 to 15%) with a length of 60m, the LS values vary from 0.1 to 5 and exceed 20 in mountainous areas, where the influence of the slope steepness is decisive. Solid transport, on the other hand, increases exponentially (exponent = ± 1.4 to 2) with the percentage of slope (Zingg, 1940; Roose, 1996).

2.3.2. Factor R: Rainfall erosivity

The kinetic energy of rain plays a significant role in the clearance of the solid particles. It is influenced by the size and velocity of raindrops and is related to the intensity of rain. Knowing the kinetic energy and average intensity of rainfall during a 30-minute is necessary to estimate the climatic aggressiveness factor using Wischmeier and Smith's (1978) model. However, only the average monthly and yearly rainfall data are available for the reference climatic stations of the Agoudal watershed, as shown in Tables 1 and 2. As a result, the equation used in Eq.3 is the following one, (Eq.3), which was created by Rango and Arnoldus (1987):

$$Ln(R) = 1.74 \times log\frac{\sum {p_i}^2}{p} \times 1.29 \quad (3)$$

Were,

pi: monthly precipitation; p: annual precipitation; R: Climatic aggressiveness

The climatic characteristics of the stations were used to estimate the erosivity values for the study area, as follows:

Table 1. Coordinates of reference rainfall stations

Stations	X	Y
M'Semrir	460759	122958
Imchil	478855	173650
Tillouguit	422674	158474
Zaouietahnsal	433362	138594

Table 2. Rainfall data from reference stations

Station	Oct.	Nov.	Dec.	Jan.	Feb.	Mar.	April	May	June	July	Aug.	Sept.	CumulAnnual
M'semrir	29.9	21.4	12.8	14.7	16.4	20.8	20.8	18	13.7	4.9	17.4	20	210.8
Imilchil	78.6	31.5	31.5	1.9	8.4	23	30.8	42.1	29.9	17.3	22.8	60.3	377.9
Tillouguite	23.8	42	39	46.6	47.5	51.5	37.1	23.7	9.7	3.5	11.5	14.7	350.5
Zaouiet Ahnsal	38.2	35.3	35.5	36	34.2	39.9	39.2	25.6	23	6.6	23.2	26.2	362.9

2.3.3. Factor C: Vegetation cover

To prevent water erosion, plant cover factor (C) is a crucial determinant of the rate of erosive activity. For well-covered soils, their values are (0.001), whereas for bare soils, they are (1), (Wischmeier and Smith, 1978). A land cover map was developed from a Landsat 8 image taken on 3/28/2021, which was previously processed using the Normalized Difference Vegetation Index (NDVI) to distinguish bare land from forested land (Jensen, 2000).

The realization of an unsupervised classification, followed by a supervised classification, made it possible to determine the distribution of vegetation cover in the study area based on the colored compositions of the image bands (bands 3, 4, and 5). NDVI is given by the following formula:

NDVI= PIR-R/PIR+R (4)

Where:

PIR: near-infrared band; **R**: red band). For the Landsat 8 version, NDVI = B5-B4/B5+B4 (where B5: Band 5 represents PIR, B4: Band 4 represents red).

2.3.4. Factor P: Cultivation practices

This parameter makes it possible to estimate soil losses in watersheds while accounting for current erosion control techniques. Depending on how well they reduce runoff and mitigate the causes of erosion, each intervention offers a certain level of protection (Brahim et al., 2020). Bench reforestation, contouring, alternating strip or terrace cropping, and ridging are among the best methods for conserving soil (Zouagui, 2018).

Both the slope and practice used affect the P-factor values. According to Shin (1999), these values are less than or equal to (1). It was the highest on land that did not employ any of the aforementioned methods. In the case of the studied basin, where the land is mainly pastoral and where cultivation practices are limited to small plots on the banks of the wadi according to our surveys, we can assign approximate values to this factor according to the type of occupation and practices used.

2.3.5. Factor K: Soil erodibility

Based on the criteria of organic matter, structure, texture, and permeability, the soil properties of the target area were interpreted and then categorized in the (Wischmeier and Smith (1978) Table to approximate the (K-factor). The absence of a soil survey in the study region makes it challenging to determine these criteria. Because the (K factor) determines the composition of soils and reflects their degree of erodibility, it is a deciding factor in the equation (Eq. 5), (Wischmeier and Smith's, 1978). Therefore, its assessment was predicated on the application of the following equation (Eq.5) to for the examination of soil samples which collected in the research region:

$$100\mathrm{K} = 2.1\mathrm{M}^{1.14} \times 10^{-4} \times (12 - \mathrm{a}) + 3.25(\mathrm{b} - 2) + 2.5(\mathrm{c} - 3) \quad (5)$$

Where:

K: Soil erodibility in ha.H/ha.MJ.mm; M: (% Fine sand +% Silt) *(100% Clay); a: % of organic matter; b: Soil structure code (1 to 4) [1: Very fine; 2: Fine; 3: Medium and coarse; 4: Very coarse]; c: Permeability code (1 to 6) [1: fast; 2: medium to fast; 3: moderate; 4: slow to moderate; 5: slow and 6: very slow].

(K-factor) values were adjusted in the study area and obtained using the following equation (Eq.6):

$$K_{adjust} = K \times (0.983 - 0.0189X + 0.0000973X\text{^}2) \quad (6)$$

Where:

K: Erodibility factor; X: Coarse surface element percentage with a size greater than 2 mm.

The evaluation of the many universal equation elements over the entire research region and their representation in the form of thematic maps were necessary for the application of this formula (Eq. 6). These maps were later included in both Quantum GIS (QGIS) and a free geographic information system (GIS).

2.3.6. Calculation of specific soil degradation

To evaluate the portion produced and conveyed to the outlet, the used (RUSLE) model could only estimate the erosion produced on the slopes. To do so, it is imperative to consider the correction factor, which is a function of the sub-basin elevation and length of the main stream. This coefficient (or delivery ratio) was defined by (Hession and Shanholz (1988) according to the following equation (Eq. 7):

$$\mathrm{DR} = 10 \times (\mathrm{D}|\mathrm{L}) \quad (7)$$

Were:

DR: Transport coefficient; D: Watershed gradient; L: Length of the main thalweg.

3. Results and Discussion

3.1. Factor (R)

Rainfall erosivity (R-factor) is one of the most fundamental and significant factors for evaluating soil erosion using mathematical models, such as RUSLE (Brahim et al., 2020; Meshram et al., 2017; 2018ab). Rainfall intensity and frequency have an impact on erosivity, which is the capacity of raindrops to separate soil particles from their original location. Therefore, accurate erosivity calculations are necessary for practical and numerical assessments of soil erosion (Patil, 2018). After calculating the (R-factor) at the reference stations according to the formula of Rango and Arnoldus (1989). Interpolation was carried out using a GIS tool to spatialize this factor over the entire Agoudal watershed. Rainfall erosivity was higher at the higher elevation stations. At Imilchil, aggressivity recorded a value of approximately 65, as shown in Table 3, which is relatively high compared to the stations of Zaouiet Ahensal and Tillouguite and even higher than that of the station of M'semrir, which hardly exceeds 34. The results are summarized in Table 3, and are illustrated in Fig. 5 as follows:

Table 3. Calculation of the R-factor in the reference stations

Stations	Coordinates		Average annual precipitation	Erosivity index
	X	Y		
M'Semrir	460759	122958	210.8	34.25
Imchil	478855	173650	377.9	65.06
Tillouguit	422674	158474	350.5	56.44
ZaouietAhnsal	433362	138594	362.9	50.94

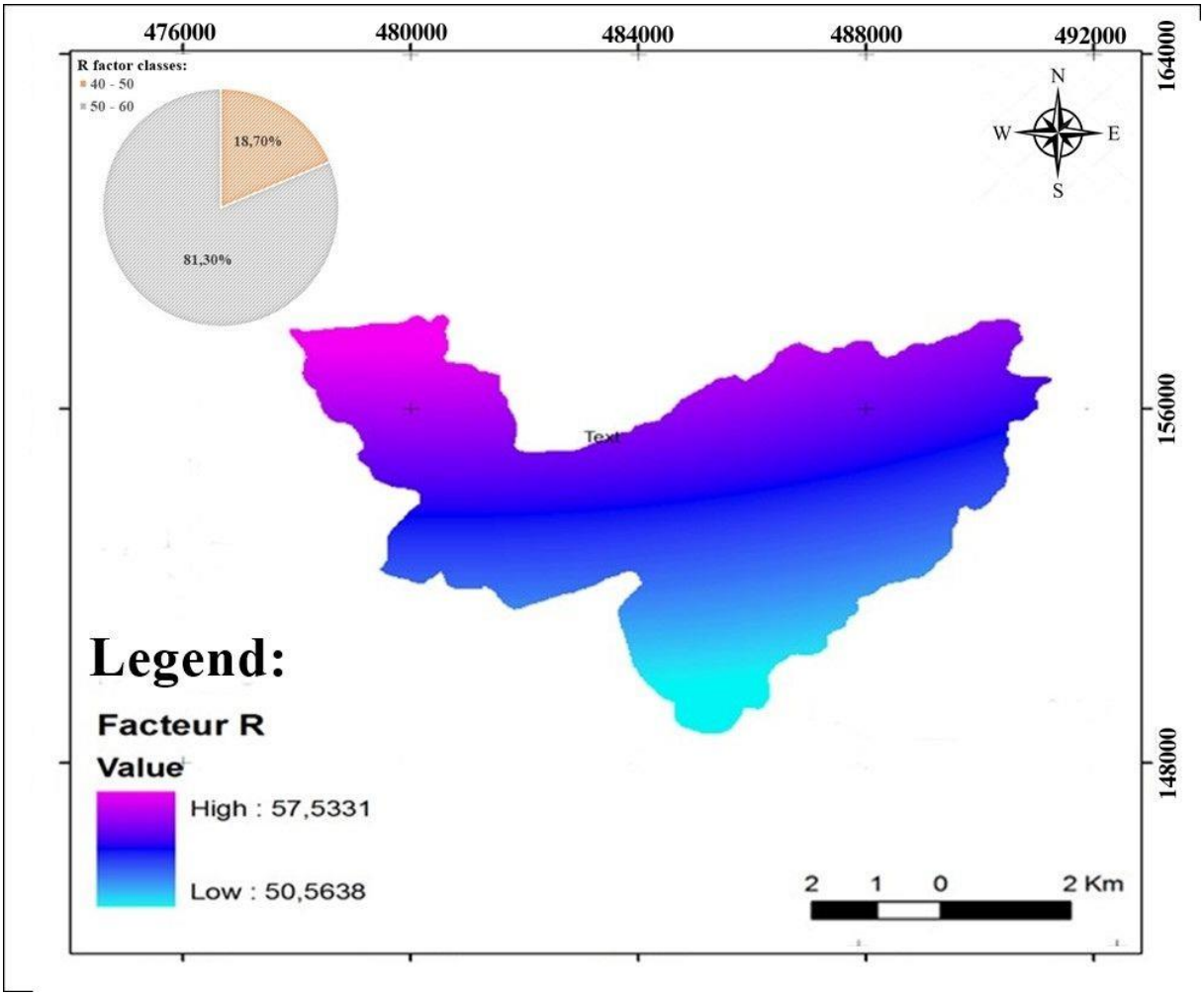


Fig. 5. R-factor map of the Agoudal Watershed

Differences in annual rainfall were followed by spatial differences in the climatic aggressiveness index. Rainfall in the study area is characterized by its torrential nature. It is poorly distributed and highly concentrated, particularly in September and October (39% of annual rainfall), at the beginning of the cropping season, when cultivated soils are poorly covered and spontaneous vegetation is very poor. Rainfall aggressiveness did not show great variability at the watershed level, but the two classes could be distinguished (Fig. 5). The first (40-50) covered less than 19% of the study area, whereas the second (50-60) dominated over 80 %. The north-facing slopes of this mountain valley, where precipitation mostly takes the form of stormy showers, particularly in the fall, have high values of this factor, indicating that it plays a significant role in creating erosive processes.

3.2. Factor LS

The topographic factor (LS) is the product of the slope length factor (L) and slope steepness/slope gradient factor (S) (Patil 2018; Brahim et al. 2020). Using terrain analysis, software extension, and GIS," the slope map in this study was created using the DEM map of the study region. Schmidt developed the following equation (Eqs. 8 and 9) in 2003, based on the fundamental research of Moore and Wilson (1992):

$$L = 1.4\left(\frac{A_{-s}}{22.13}\right)0.4 \text{ and } S = \left(\frac{\text{Sin}\beta}{0.0896}\right)1.3 \quad (8)$$

Where:

- A_s: specific watershed area per unit width (m2/m) and β is the slope angle (degrees).

$$LS = \left(\text{FlowAcc}\left(\text{FlowDir}(\text{DEM})\right)\right) \times \left(\frac{\text{Resolution}}{22.1}\right)0.4 \times \left(\text{Sin}\left(\text{Slope} \times 0.\frac{01745}{0.09}\right)1.13 \quad (9)$$

Where:

- Flow Acc and Flow Dir: are two functions integrated in the GIS software used in this study.

In the study area, the slopes are steep and not very long because of the folding of the landforms, alternating hard and soft layers that dominate the watershed landscape. With an average of approximately 40 (39.900), the LS factor values range from 2.7 to 200, and the highest value was recorded, as listed in Table 4. The other attributes are as follows:

Table 4. Topographic factor characteristics in the study area

Parameters	Values
Number of units	27626
Minimum value	2.697
Maximum value	199.871
Mean Value	39.900
Standard deviation	36.637

Specialization of this factor shows that most of the studied watersheds have values close to 40, while very high values are marked on steep slopes, where the inclination far exceeds 45%. The analysis of slope classes (Fig. 6) shows that very steep slopes of more than 45% are observed on steep reliefs and cliffs present in several places in this watershed, where 27% of its total surface is included in this range. A class of less than 5% is weakly represented and corresponds to lowlands and talwegs.

3.3. Factor C

The ratio of soil loss from an area with designated cover and management to soil loss from an equivalent area that has been kept fallow for a long time is known as the (C-factor). It evaluates how canopy and ground cover affect runoff hydraulics and raindrop impact, and how cover and management

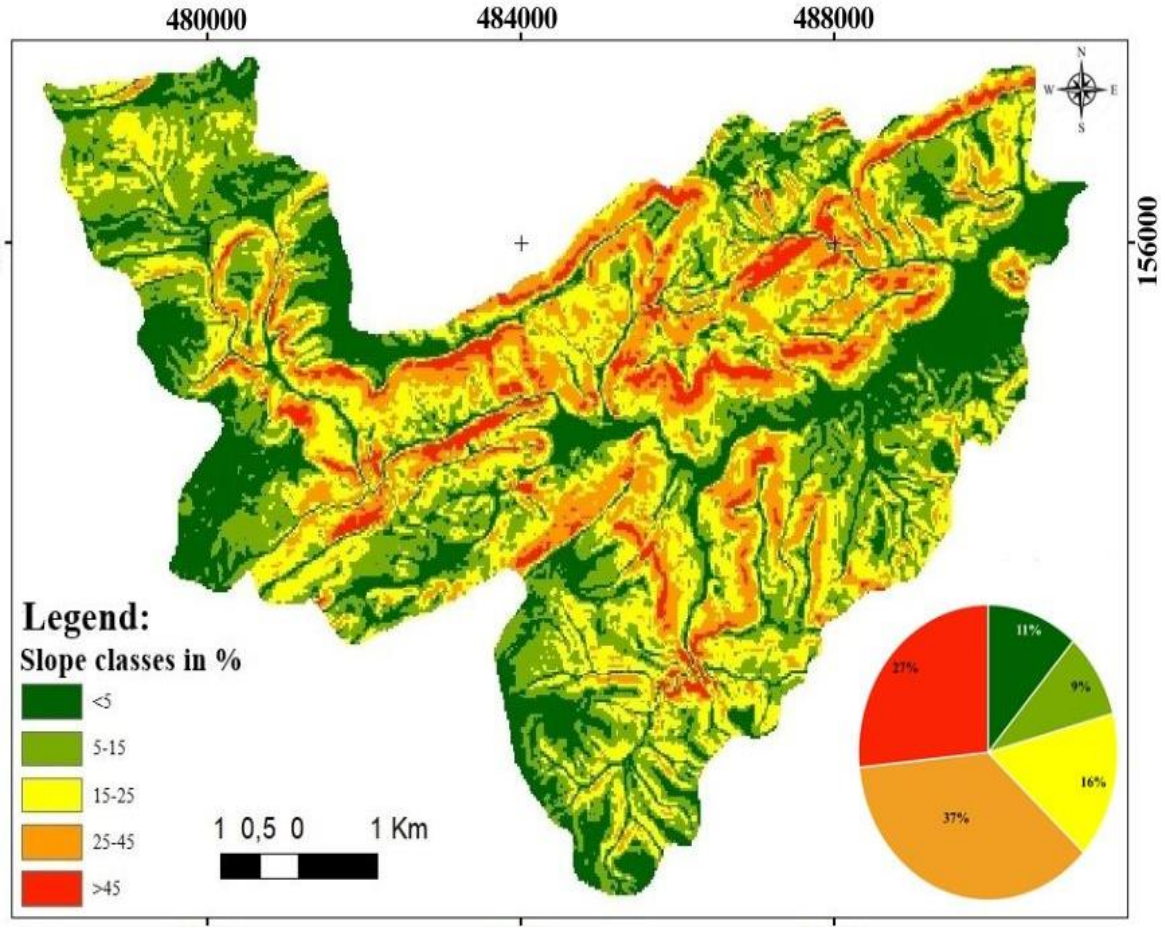


Fig. 6. Slope classes (%) of the Agoudal watershed

affect the runoff rate and volume. The (C-factor), belowground biomass, plants, soil cover, and soil-disturbing activities all affect soil erosion (Jones et al., 1996).

Because water erosion is a result of improper land use, it should be prioritized in accordance with current demands for sustainable agriculture (Desilva et al., 2010). The combination of land cover and cover rate in the study area with the characteristics of cultivation practices, allowed us to establish the characteristics of factor C (Tables 5 and 6, and Figs. 7 and 8). The numbers listed in Table 5 reveals that the average (C-factor) is quite high at (0.65). This is because of the poor protection of the soil by vegetation cover and the degradation of pastoral lands.

Table 5. Characteristics of canopy factor C in the study area

Parameter	C-factor values
Minimum value	0.25
Maximum value	1
Mean Value	0.65
Standard deviation	0.3

The very low annual cover and low-density rangeland class extend over 70% of the study area, resulting in poor soil protection from water erosion Table 6. The second is the class with xerophyte-based vegetation cover, which occupies approximately 27%. Only a small area of approximately 1.4% of the watershed of Agoudal, which has an average to good vegetation cover with values of the C factor of less than 0.25, 0.3 represented by the last two classes that correspond in the field to the small agricultural plots along the bed of the Oued d'Assif Melloul Table 6.

Table 6. Distribution of land use classes and C factor

Types of land use	C-Factor	Surface (%)
Constructions	1	0
Parkland with xerophyte-based vegetation cover	0.8	26.9
Wadi bed rangeland with very low soil cover	0.95	0.9
Very low annual cover rangeland with low density	0.9	70.8
Irrigated agricultural land with good soil cover	0.25	0.8
Irrigated agricultural land with average semi-annual cover	0.35	0.6

The steppes of xerophytes abundant in the study area are characterized by their annual aerial parts, but their root systems, which are quite developed and perennial, could logically constitute a framework for the substrate and strengthen its resistance to water erosion. However, these steppe formations are also victims of massive deforestation by local populations to meet their main daily needs, such as cooking, shower water heating, and habitat heating in cold periods. This negatively impacts the coverage and protection of soils that are already poorly covered.

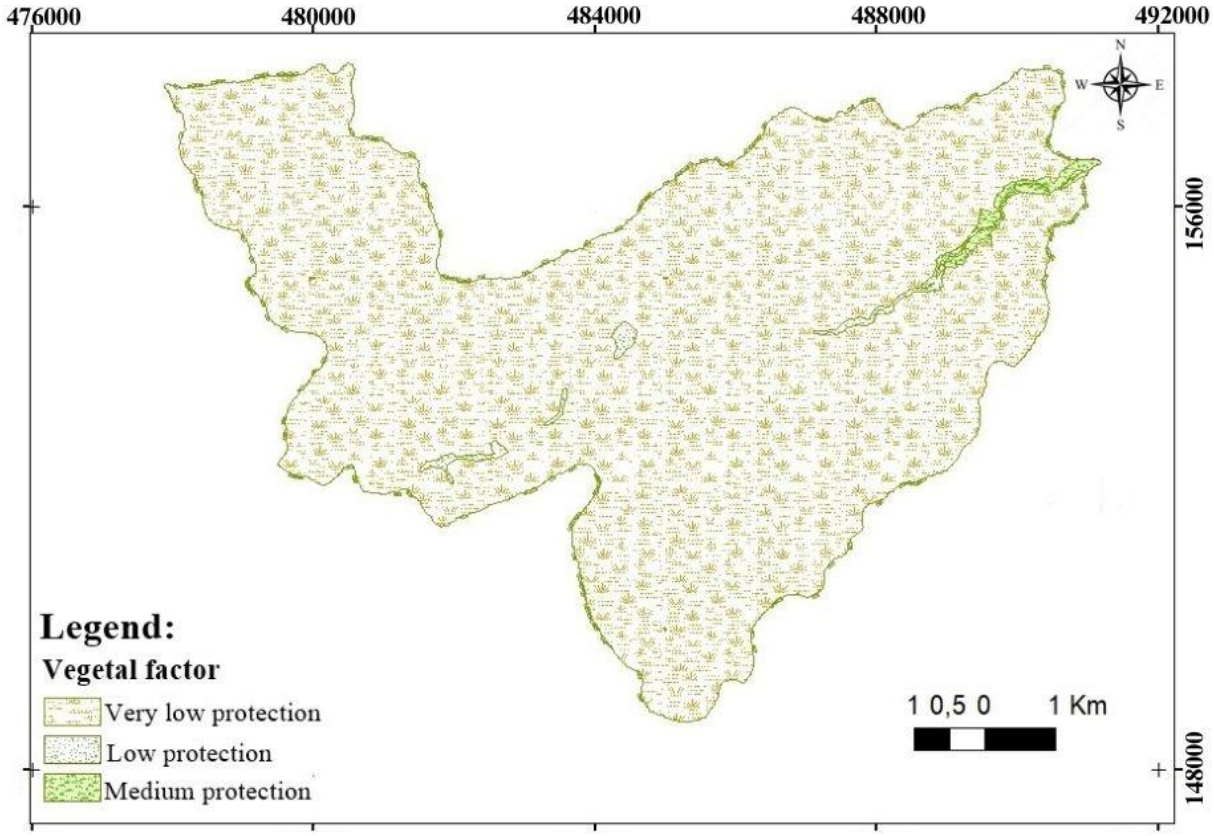


Fig. 7. C-factor map of the Agoudal Watershed

3.4. Factor P

If all other factors remain the same, the conservation or support practice factor (P) is the ratio of soil loss from a piece of land with designated conservation practices to that from a piece of land plowed parallel to a slope (Wischmeier and Smith, 1978).

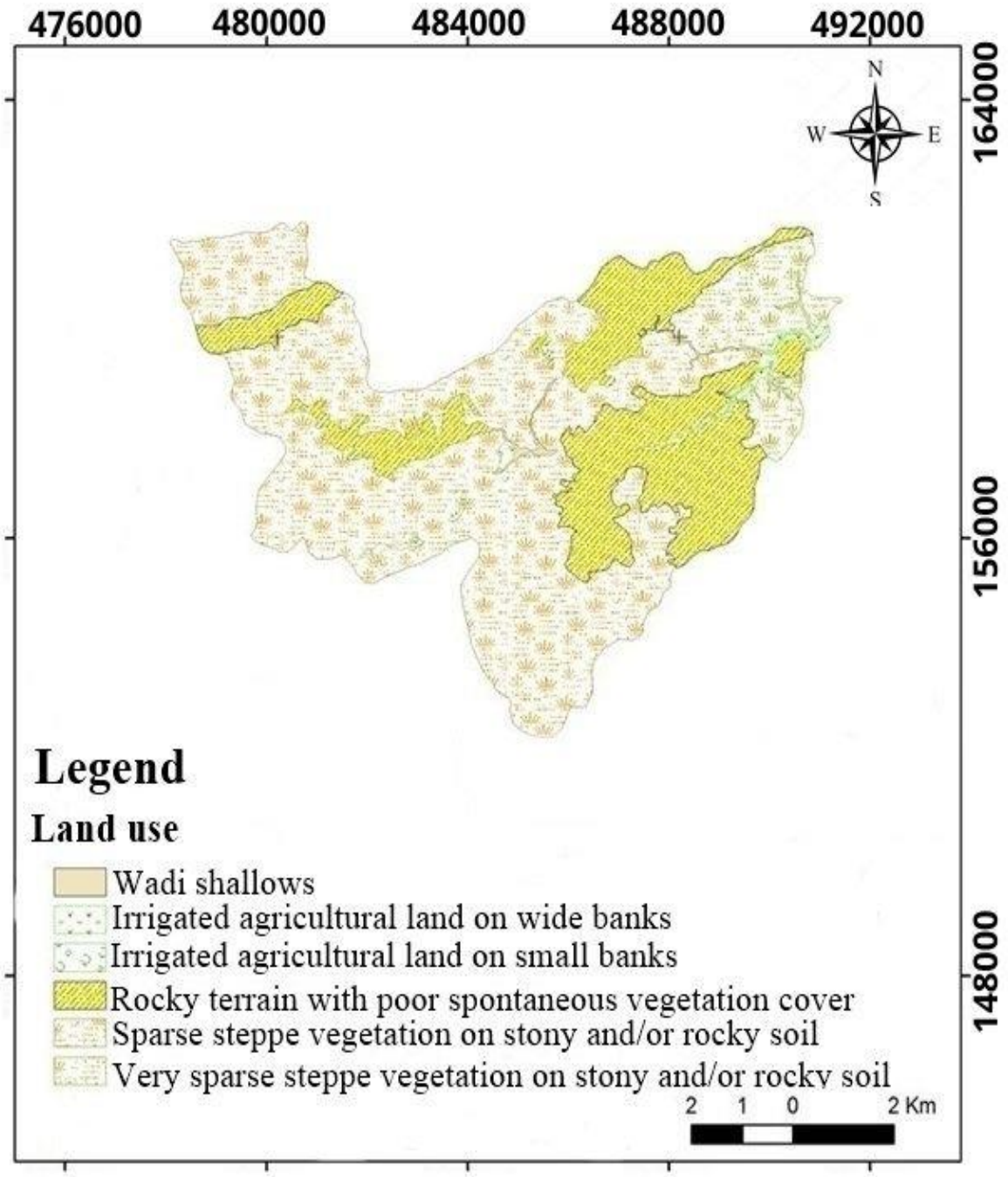


Fig. 8. Land use map of the Agoudal watershed

According to the different farmed lands on Earth, the support practice factor shows the rate of soil loss (Patil 2018). This factor makes it possible to estimate soil losses while accounting for the current erosion control techniques. The degree of protection offered by each intervention is determined by how well it reduces or mitigates sources of erosion.

The results of this factor show that (P) values ranged from 0.7 to 0.9, corresponding to fairly well to poorly protected land. These covered less than 1.5% of the area of the SBV studied, while more than 98% of these lands with a (P) value equal to 1 (Brahim et al., 2020; Shin, 1999) were without protective measures (Table 7).

Table 7. Distribution of P-factor classes in the Agoudal Watershed

Type of Practices	P index	Area (%)
Fairly protective practices	0.7	0.8
Poorly protective practices	0.9	0.6
No protective practices	1	98.6

3.5. Factor (K)

Preliminary data on the erodibility characteristics of the Agoudal watershed soils are shown in Table 8 were obtained by applying the equation proposed by Wischmeier and Smith (1978).

Table 8. Soil erodibility factor characteristics

	K-values
Minimum value	0.1400
Maximum value	0.4576
Average Value	0.3970
Standard deviation	0.0793

Preliminary erodibility values (Fig. 9) reveal that the (K) class of 0.36 to 0.4, which includes erodible soils, represents 80% of the area of the Agoudal watershed with an average of over 0.39 (Table. 8) as shown above.

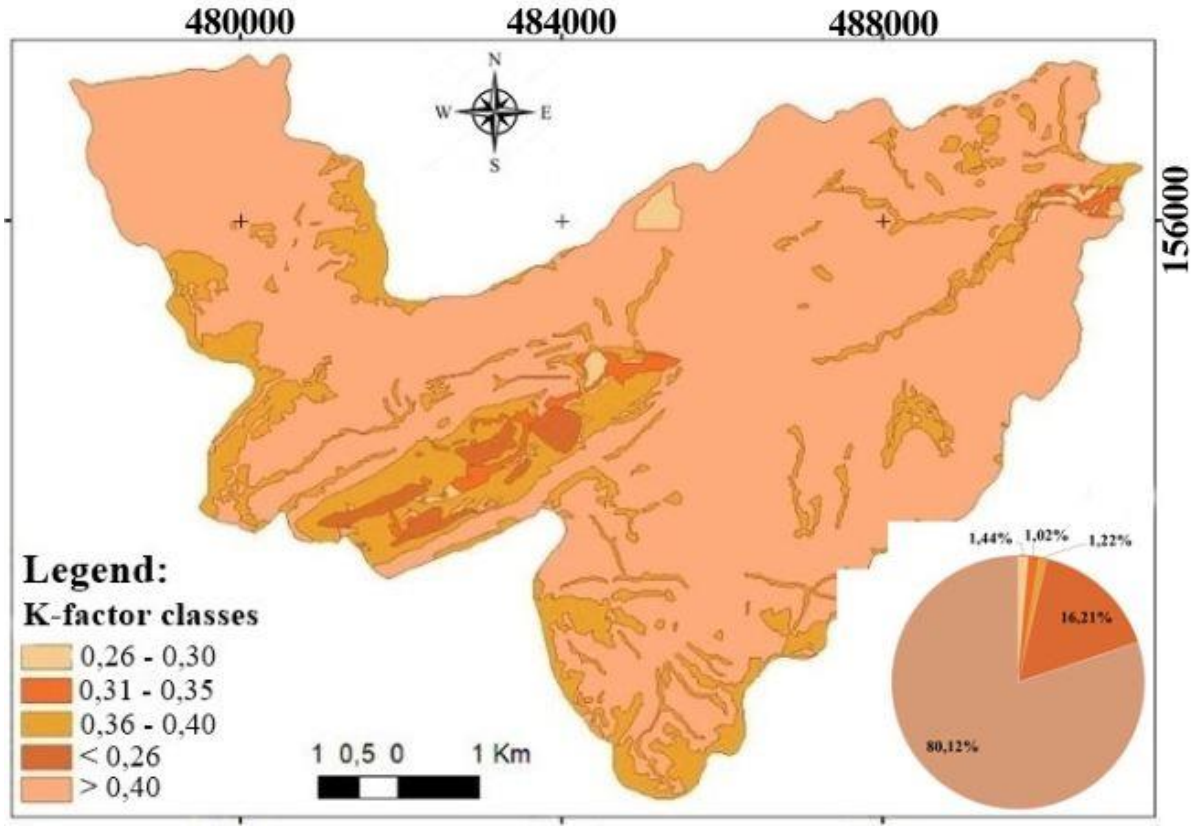


Fig. 9. Map and proportion of K-factor classes in the Agoudal watershed

During the field surveys, the presence of coarse elements was noted in areas with multiple rocky outcrops on the slopes, particularly on the calcareous and marly calcareous summits. These outcrops are

carried towards the mid and low slopes by erosive processes, becoming the predominant elements on the surface of the watershed. For this situation, it proceeded to adjust the value of factor K, as given in (Eq. 5) above.

The adjusted erodibility factor classes represent the highest friability, which is (>0.2), covering 8% of the study area, giving way to the less erodible classes (Fig.10). These changes in rates revealed after adjusting for the (K-factor), can be explained by the dominance of coarse elements covering the majority of the landscape of the study area, which is consistent with field surveys and soil particle size analyses.

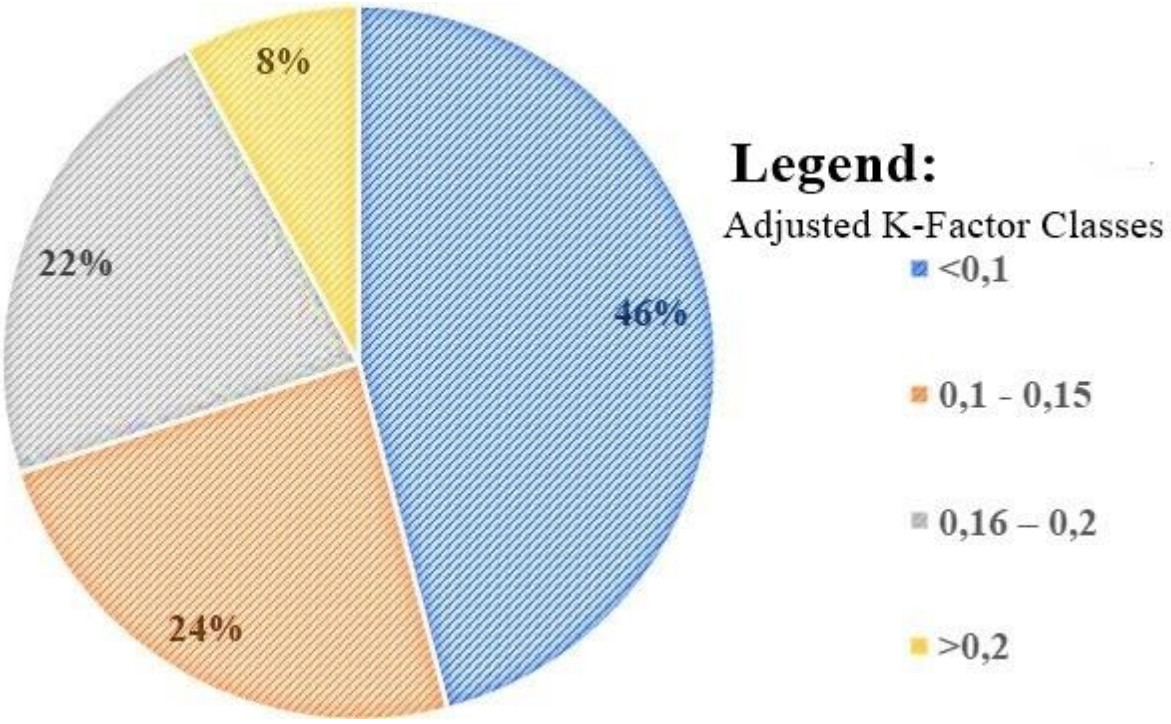


Fig. 10. Class distribution of adjusted K-factor

3.6. Soil Loss Assessment

Wischmeier and Smith's (1978) empirical model has several limitations of fit under conditions that differ from those in which it was developed. It assumes that all surfaces are subject to erosion if none of the factors are zero, that is, it does not account for both slope and fluvial deposits. The evaluation of the causative variables and their spatialization over the entire watershed under study was made possible by the outcomes of using this model after the five components were modeled in thematic maps using GIS. The average field erosion value obtained was 255.058 t/yr/ha, with a standard deviation of less than 285 t/yr/ha (Table. 9) in response to environmental heterogeneity and conditions.

Table 9. Characteristics of erosion classes in the Agoudal watershed

Soil Erosion	Values in t/ha/year
Minimum value	1.223
Maximum value	1987.730
Average Value	255.058
Median	154.680
Standard deviation	284.967

These values seem, at first glance, a little high, but reality shows that these processes are all more active as the soils have undergone profound changes in their structures, which have induced generalized slippage over time. Hence, the outcrop of bedrock on almost all the slopes of the watershed, where large bare land stripped of soils is abundant with outcrops of skeletal rocks, including gullies, testifies to the rapid evolution of this scourge in these very vulnerable ecosystems where all factors are combined to accelerate erosion rates. The data are reported in Table. 10, show that the classes 50 to 400 t/ha/year are the most represented and cover about 66% or the erosion rate in two-thirds of the studied area is extremely high, reaching a maximum of 1987.73 t/ha/year and an average of around 255 t/ha/year with a standard deviation of roughly 285 t/ha/year, as shown in Table. 9 above. This rate is far from being tolerated by soils that suffer, in addition to the lack of plants, an aggressive climate with rainfall of a stormy nature very localized in time and space.

Table 10. Erosion classes in the field in the Agoudal watershed

Degree of erosion (t/ha/yr)	Area in (%)	Cumulative area (%)
<50	18,1	18,1
50-100	20,2	38,3
101-150	14,8	53,1
151-200	11	64,1
201-300	11,7	75,8
301-400	7,8	83,6
401-500	4,5	88,1
501-1000	7,1	95,2
>1000	4,8	100

Fig**.** 11 thus far exceeds what pedogenesis can produce to compensate for these losses, the consequences of which include a drop in crop yields and a reduction in the surface area of useful Agricultural Areas (UAA) concentrated on the banks of the river. These results are generally higher than those reported in previous studies in other regions of the High Atlas (Simonneaux et al., 2015; Bou-Imajjane et al., 2020), where soil loss classes were between 50 and 400 t/ha/year, covering approximately half of the areas studied. The cases of Oum Er-Rabia and Ourika affect 54% in the first case (Yjjou et al., 2014) and 48% in the second case (Meliho et al., 2016).

3.7. Specific Degradation

The results obtained after correction (Table 11 and Fig. 11) correspond to the specific degradation of the watershed, which shows that the majority of its area is subject to very strong degradation beyond the soil tolerance threshold.

Table11. Erosion rates in the field in the Agoudal watershed

L(m)	D(m)	DR	Specific degradation (t/h/year)			Total loss (t/year)
			Min	Max	Average	
18485	700	0,38	0,46	755,3	96,9	605528

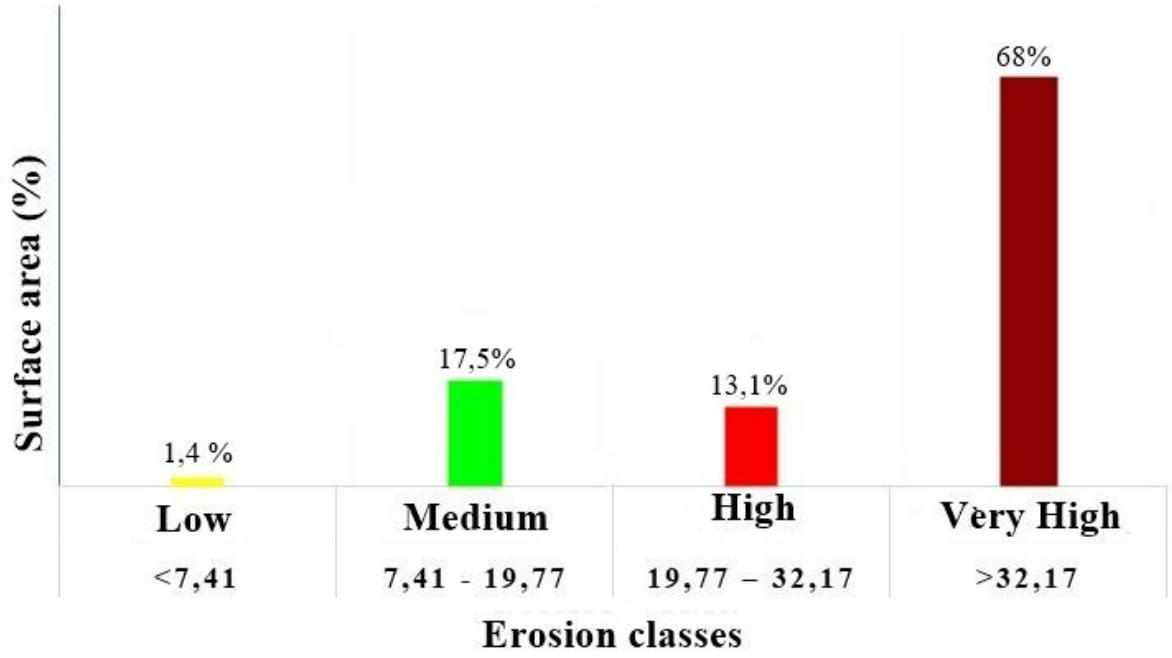


Fig. 11. Degree of specific degradation in the study area

Only 18.9% of the watershed's total area exhibits low- and medium-degree erosion rates, and less than 1.5% of the studied area is susceptible to erosion rates of less than 7.4 t/ha/yr. These areas correspond to the zones that lengthen the main watercourses and correspond to the low-lying areas located on slopes of less than 15%, with the remarkable presence of coarse elements offering a certain protection that lessens the effect of raindrops and attenuates the runoff's kinetic energy.

The impact of each factor in the erosion equation was different. In fact, the topographic factor and erodibility factor in this area are revealed to be two important variables in the sensitivity to erosion, since the rates of soil degradation are proportional to them. However, the length and inclination of the slope are not good indicators, as the highest erosion rates were recorded in the LS classes between 15 and 25%.

After analyzing the various causal factors of erosion, the findings were contrasted with the official data gathered (topographical and geological maps of the research region, climate data, and erosion studies conducted by the relevant state departments), and with the actual conditions on the ground, we mapped the zones that are vulnerable to the processes of erosion and soil degradation (Fig. 12). Such a result could, in our opinion, be useful to the different public operators involved, to the actors of civil society, and to all the stakeholders involved in the process of erosion control, especially in the planning of operations for the protection of the soil and the microbiological, rhizospheric, and pedological resources in this very needy mountainous area.

Four levels of vulnerability were identified and spatialized to visualize the priority sites at risk of degradation that could be used in the case of possible interventions within the framework of the development programs of the watershed of Agoudal upstream of the valley of Imilchil. These areas were identified based mainly on an average erosion rate of 255.058 t/ha/year (Table 9) and specific degradation classes. Only 1.4% of the Agoudal watershed exhibits rates below 7.4%, and 68% of the entire region is susceptible to degradation rates higher than 32.7% (Fig. 11). This prioritization was done to frame vulnerable and potentially developable areas to reduce erosion and flood generation, and to protect downstream settlements and infrastructure.

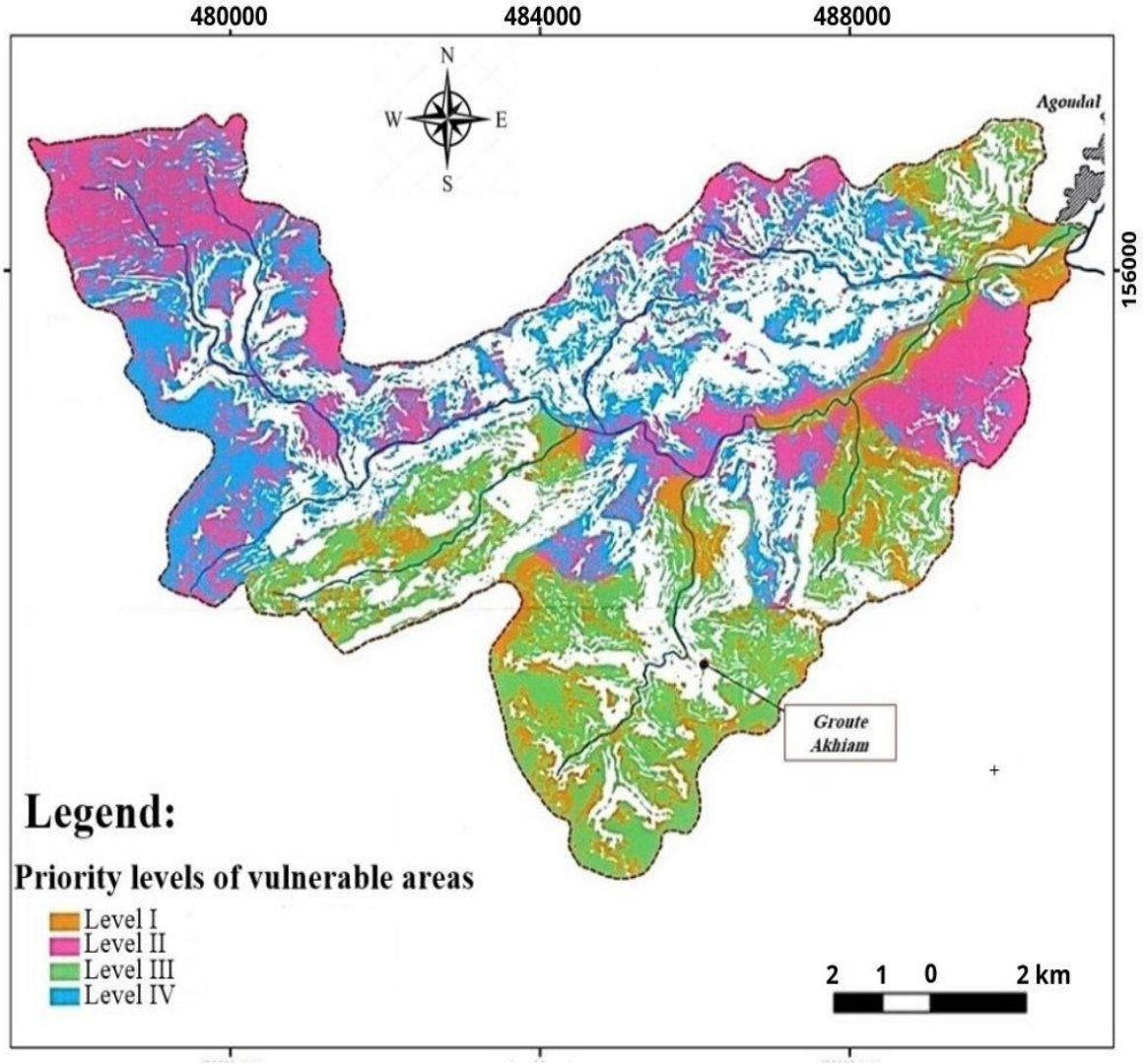


Fig. 12. Map of vulnerable areas and their priority levels in the Agoudal Watershed

To better frame the interventions for the mitigation of erosive effects and floods, it was necessary to synthesize a map spatializing the intervention areas, considering the characteristics of the hydrographic network developed by Archydro (ArcGis) and the map of priority vulnerable areas previously developed (Fig. 12). This led to the delineation of intervention areas and the definition of adequate mitigation measures to ensure the protection of habitats, farms, and crops of riparian populations, mitigate the effects of floods and torrential floods on habitats and agricultural land, and contribute to the preservation of soil resources and biodiversity. Mitigate erosion processes, slope gullies, and bank scarping.

To act more effectively, it is necessary to consider the characteristics of the network to target the areas to be stabilized in order to mitigate the harmful effects of floods. It is also necessary to combine mechanical interventions with biological actionsto achieve greatere sustainability. The erosion control map (Fig. 13) shows the geographical locations of the main management measures and actions proposed for the Agoudal sub-watershed based on an evaluation study of erosive processes. Some of the proposed interventions were also valid for similar watersheds.

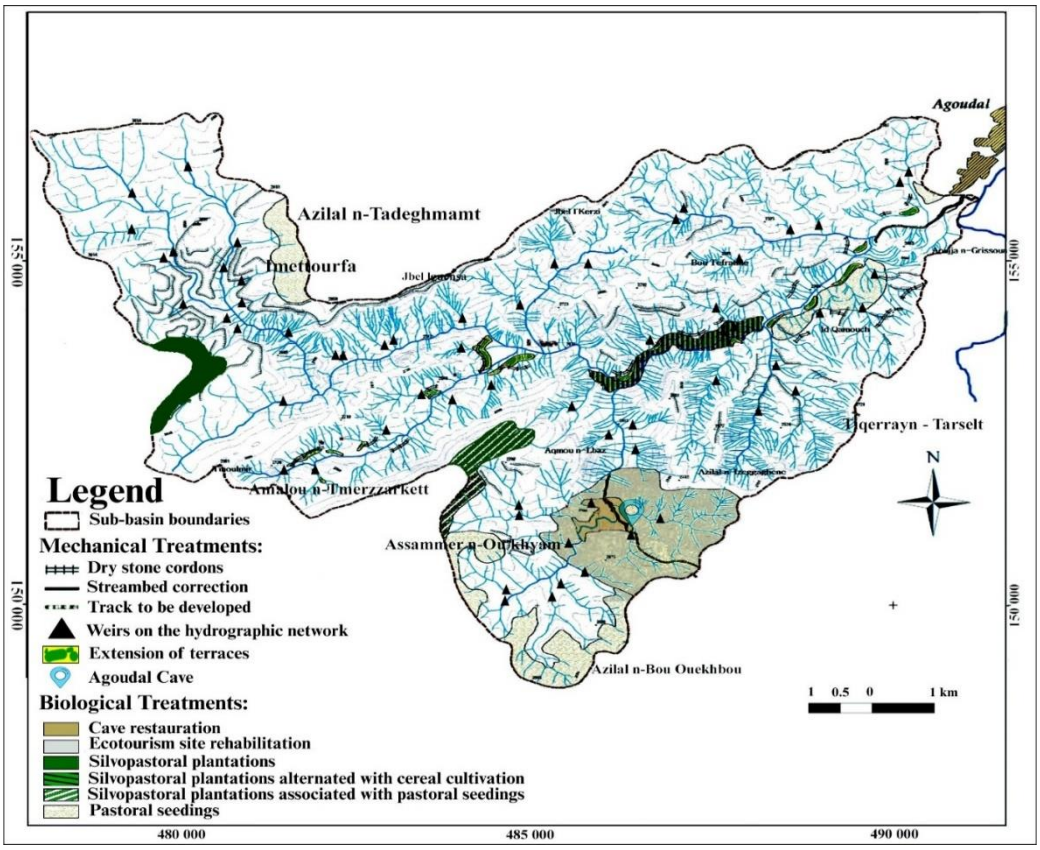


Fig. 13. Map of anti-erosion development of the Agoudal watershed

4. Conclusions

- The results obtained in the framework of the present work affirm that the study area is threatened by the phenome of water erosion and the continuous degradation of the quality of the soils, whose consequences impact negatively the sustainable development of this region
- One of the many drawbacks of the used (RUSLE) model is that, because it uses rain as its energy source, it only applies to groundwater erosion. To distinguish the effects of each of the components more clearly, it ignores some of their interactions and only applies to average data spanning at least 20 years, never to linear or mass erosion.
- According to the methodology, the watershed under study faces the threat of water erosion, which affects over 98% of its total area, with 68% of the area experiencing very high specific degradation exceeding 32.17 t/ha/year. The average rate of water erosion exceeds 255 t/ha/year, and the specific degradation rates exceed 7.41 t/ha/year. The exploitation of these results has led us to identify and prioritize the areas at risk in the Central Atlas, in this case, the watershed of Agoudal upstream of the basin of Oum Er-Rbia. This can serve as a model and be generalized to the watershed of Assif Melloul, which constitutes its downstream continuity and suffers from the same problem. It can be transposed to other regions of the Central High Atlas because of the similarities in their geomorphological, geological, pedological, edaphic, and climatic characteristics. Thus, the combined map of erosion vulnerability might serve as a foundational document for any upcoming management and development initiatives and activities aimed at reducing this scourge and its detrimental effects on the operation of agropastoral ecosystems in

the area. Radioactive indicators such Cesium 137 (137Cs), EPM, and PAP/CAR, must be analyzed to determine the rate of soil loss in the Agoudal watershed.

References

Amrhar, M., 1995. Tectonique et inversions géodynamiques post-rift dans le Haut-Atlas occidental : structures, instabilités tectoniques et magmatismes liés à l'ouverture de l'Atlantique central et la collision Afrique-Europe. Doctorat thesis, University of Marrakech, Morocco, 253.

Anys, H., Bonn, F., Merzouk, A., 1994. Remote sensing and GIS based mapping and modeling of water erosion and sediment yield in a semi-arid watershed of Morocco. Geocarto International, 9(1): 31-40.

Anys, H., Bonn, F., Merzouk, A., 1992. Cartographie et calcul de l'érosion hydrique à l'aide de télédétection et du SIG, cas du bassin versant d'oued Aricha (Settat, Maroc), Géo Observateur, 2:37-51.

Badraoui, A., Hajji, A., 2001. Envasement des retenues de barrages. La Houille Blanche (6-7): 72-75.

Batista, PVG., Davies, J., Silva, MLN., Quinton, JN., 2019 On the evaluation of soil erosion models: are we doing enough. Earth Sci. Rev., 197 https://doi.org/10.1016/j.earscirev.2019.102898

Benbrahim, KF., Ismaili, M., Benbrahim, SF., Tribak, A., 2004. Problèmes de dégradation de l'environnement par la désertification et la déforestation : impact du phénomène au Maroc. Science et changements planétaires/Sécheresse, 15(4): 307-320.

Bennmoussa, M., Elyamani, M., Saidi, A., 1993. Application de l'équation universelle des pertes en sols au bassin versant d'Oued Tasrafate, Géo Observateur, 3 :83-93

Benzougagh, B., Meshram, SG., Dridri, A., Boudad, L., Baamar, B., Sadkaoui, D., Khedher, KM., 2022. Identification of critical watershed at risk of soil erosion using morphometric and geographic information system analysis. Applied Water Sci, 12(1): 1-20. https://doi.org/10.1007/s13201-021-01532-z

Benzougagh, B., Meshram, S.G., Fellah, B.E. et al. 2023. Mapping of land degradation using spectral angle mapper approach (SAM): the case of Inaouene watershed (Northeast Morocco). Model. Earth Syst. Environ. https://doi.org/10.1007/s40808-023-01711-8

Borrelli, P., Van Oost, K., Meusburger, K., Alewell, C., Lugato, E., Panagos, P., 2018. A step towards a holistic assessment of soil degradation in Europe: coupling on-site erosion with sediment transfer and carbon fluxes Environ. Res., 161: 291-298, https://doi.org/10.1016/j.envres.2017.11.009

Boudhar, A., Duchemin, B., Hanich, L., Chaponnière, A., Maisongrande, P., Boulet, G., Chehbouni, A., 2007. Analyse de la dynamique des surfaces enneigées du Haut Atlas marocain à partir des données SPOT-VEGETATION. Science et changementsplanétaires/Sécheresse, 18(4): 278-288.

Bou-Imajjane, L., Belfoul, M. A., 2020. Soil loss assessment in western high Atlas of Morocco: Beni Mohand watershed study case. Applied and Environmental Soil Science, 2020(1), 6384176. https://doi.org/10.1155/2020/6384176

Brahim, B., Meshram, SG., Dridri, A., Boudad, L., Sadkaoui, D., Mimich, K., Khedher, KM., 2020. Mapping of soil sensitivity to water erosion by RUSLE model: case of the Inaouene watershed (Northeast Morocco). Arabian Journal of Geosciences, 13: 1153. https://doi.org/10.1007/s12517-020-06079-y

Charrière, A., Haddoumi, H., Mojon, PO., Ferrière, J., Cuche, D., Zili, L., 2009. Mise en évidence par charophytes et ostracodes de l'âge Paléocène des dépôts discordants sur les rides anticlinales de la région d'Imilchil (Haut Atlas, Maroc) : conséquences paléogéographiques et structurales. Comptes Rendus Pale, 8(1) : 9-19.

Charrière, A., Haddoumi, H., 2016. Les «Couches rouges» continentales jurassico-crétacées des Atlas marocains (Moyen Atlas, Haut Atlas central et oriental) : bilan stratigraphique, paléogéographies successives et cadre géodynamique. Boletíngeológico y minero, 127(2-3), 407-430.

Choubert, G., Faure-Muret, A., 1960. Evolution du domaine atlasique marocain depuis les temps paléozoïques. Mémoire hors-série-Société géologique de France (1) : 447-527.

Croitoru, L., Sarraf, M., 2017. Le Coût de la Dégradation de l'Environnement au Maroc. Environment and Natural Resources Global Practice Discussion Paper, 5.

Desilva, RP., Dayawansa, NDK., Jayarathne, KDBL., 2010. GIS-based analysis of biophysical and socio-economic factors for land degradation in Kandaketiya DS division. Tropical Agric Res 21(4):361–367.

Elalaoui, A., Marrakchi, C., Fekri, A., Maimouni, S., Aradi, M., 2015. Mise en place d'un modèle qualitatif pour la cartographie des zones à risque d'érosion hydrique dans la chaîne atlasique : cas du bassin versant de la Tessaoute amont. (Haut Atlas Central, Maroc). Eur Sci J 11(29), 106–121.

El Garouani, A., Merzouk, A., Ozer, A., 2003. Cartographie et évaluation quantitative de l'érosion hydrique au Prérif marocain. IAHS Publication, Wallingford, 380–388

El Garouani, A., Merzouk, A., Jabrane, R., Boussema, MR., 2005. Analyse spatiale de l'érosion en nappe et de l'infiltrabilité des sols dans le PréRif marocain. Télédétection 5(1-2-3) : 69–80

El Garouani, A., Chen, H., Lewis, L., Tribak, A., Abharour, M., 2008. Cartographie de l'utilisation du sol et de l'érosion nette à partir d'images satellitaires et du sigidrisi au nord-est du maroc. Télédétection 8(3) :193–201.

Froitzheim, N., Stets, J., Wurster, P., 1988. Aspects of western High Atlas tectonics. In The Atlas System of Morocco 219-244. Springer, Berlin, Heidelberg.

Hession, WC., Shanholtz, VOA., 1988. Geographic information system for targeting nonpoint-source agricultural pollution. Journal of Soil and Water conservation, 43(3):264-266.

Ibouh, H., Chafiki, D., 2017. La tectonique de l'Atlas : ageetmodalit es. Le Maroc, paradis des g eologues:Soci et egeologue de France 194.

Issa, LK., Lech-Hab, KBH., Raissouni, A., El Arrim, A., 2016. Cartographie quantitative du risque d'erosion des sols par approche SIG/USLE au niveau du bassin versant Kalaya (Maroc Nord Occidental). J Mater Environ Sci 7(8) : 2778–2795.

Jenny, J., Le Marrec, A., Monbaron, M., 1981. Les couches rouges du Jurassique moyen du Haut Atlas central (Maroc) ;Correlations litho-stratigraphiques, elements de datations et cadre tectono-sedimentaire. Bulletin de la Société géologique de France, 7(6) : 627-640.

Jones, RJA., Montanarella, L., Van der Knijff, JM., 1996. Soil erosion risk assessment in Italy. Space Applications Institute, European Soil Bureau.

Jensen, JR., 2000. Remote Sensing of the Environment an Earth Resource Perspective Prentice Hall. upper Saddle River (NJ), USA.

Keesstra, S., Nunes, JP., Saco, P., Parsons, T., Poeppl, R., Masselink, R., Cerdà, A., 2018. The way forward: can connectivity be useful to design better measuring and modelling schemes for water and sediment dynamics. Sci. Total Environ., 644: 1557-1572, https://doi.org/10.1016/j.scitotenv.2018.06.342

Lal, R., 2019. Accelerated Soil erosion as a source of atmospheric CO 2 Soil Tillage Res., 188: 35-40, https://doi.org/10.1016/j.still.2018.02.001

Laville, E., Lesage, JL., Seguret, M., 1977. Geometrie, cinematique (dynamique) de la tectonique atlasique sur le versant sud du Haut Atlas marocain ; apercu sur les tectoniques hercyniennes et tardi-hercyniennes. Bulletin de la Société géologique de France, 7(3) : 527-539.

Lizaga, I., Gaspar, L., Blake, WH., Latorre, B., Navas, A., 2019. Fingerprinting changes of source apportionments from mixed land uses in stream sediments before and after an exceptional rainstorm event Geomorphology, 341: 216-229, https://doi.org/10.1016/j.geomorph.2019.05.015

Lugato, E., Paustian, K., Panagos, P., Jones, A., Borrelli, P., 2016. Quantifying the erosion effect on current carbon budget of European agricultural soils at high spatial resolution Global Change Biol., 22: 1976-1984, https://doi.org/10.1111/gcb.13198

Meliho, M., Abdellatif, K., Nadia, M., Zhang, H., 2016. Cartographie Des Risques De L'érosion Hydrique Par L'équation Universelle Révisée Des Pertes En Sols, La Télédétection Et Les SIG Dans Le Bassin Versant De L'Ourika (Haut Atlas, Maroc). Eur Sci J 12(32) : 227-297.

Merkhi, A., Laftouhi, NE., Soulaimani, A., Fniguire, F., 2015. Quantification et évaluation de l'érosion hydrique en utilisant le modèle RUSLE et dépositions intégrées dans un SIG. Application dans le bassin versant n'fis dans le haut atlas de Marrakech (Maroc). Eur Sci J 11(29), 340– 356.

Meshram, SG., Powar, PL., Singh, VP., 2017. Modelling soil erosion from awatershed using cubic splines. Arab J Geosci 10:155–168. https://doi.org/10.1007/s12517-017 2908-1

Meshram, SG., Powar, PL., Singh, VP., Meshram, C., 2018a. Application ofcubic spline in soil erosion modelling from Narmada Watersheds,India. Arab J Geosci 11:362. https://doi.org/10.1007/s12517-018-3699-8

Meshram, SG., Powar, PL., Meshrm, C., 2018b. Comparasion of cubic,quadratic and quintic splines for soil erosion modelling. Appl Water Sci 8:173. https://doi.org/10.1007/s13201-018-0807-6

Michard, A., Ibouh, H., Charri ere, A., 2011. Synclinetopped anticlinal ridges (STARs) from the High Atlas: A Moroccan conundrum, and inspiring structures from the Syrian Arc, Israel. Terra Nova. 23 :314–323.

Mitasova, H., Hofierka, J., Zlocha, M., Iverson, LR., 1996. Modelling topographic potential for erosion and deposition using GIS. International journal of geographical information systems, 10(5): 629-641.

Moore, I. D., Wilson, J. P., 1992. Length-slope factors for the Revised Universal Soil Loss Equation: Simplified method of estimation. Journal of soil and water conservation, 47(5), 423-428. https://doi.org/10.1080/00224561.1992.12456740

Mrabet, R., Acherkouk, M., Maatougui, A. 2020. "La fertilisation améliore la production des prairies humides naturelles dans la montagne du haut Atlas oriental du Maroc : cas de la région d'Imilchil." African and Mediterranean Agricultural Research Journal-Al- Awamia (128).

Ouadjane, Y., Ait Yacine, E-A., Benzougagh, B., Nassiri, L. Ibijbijen J., 2021. Evaluation Des Risques D'érosion Hydrique Et Cartographie Des Zones Vulnérables Par La Méthode RUSLE Couplée Aux SIG Et À La Télédétection Dans Le Bassin Versant d'Agoudal En Amont De La Vallée d'Imilchil (Haut Atlas Central, Maroc). European Scientific Journal, ESJ, 17(21), 66. https://doi.org/10.19044/esj.2021.v17n21p66

Ouallali, A., Moukhchane, M., Aassoumi, H., Berrad, F., Dakir, I., 2016. The mapping of the soils' degradation state by adaptation the PAP/RAC guidelines in the watershed of Wadi ArbaaAyacha, Western Rif, Morocco. J Geosci Environ Prot, 4(07) :77–82.

Panagos, P., Katsoyiannis, A., 2019. Soil erosion modelling: the new challenges as the result of policy developments in Europe Environ. Res., 172: 470-474, https://doi.org/10.1016/j.envres.2019.02.043

Patil, RJ., 2018. Spatial techniques for soil erosion estimation: remote sensing and GIS approach. Springer International Publishing. https://doi.org/10.1007/978-3-319-74286-1

Quinton, JN., Govers, G., Van Oost, K., Bardgett, RD., 2010. The impact of agricultural soil erosion on biogeochemical cycling Nat. Geosci., 3: 311-314, https://doi.org/10.1038/ngeo838

Rango, A., Arnoldus, HMJ., 1987. Aménagement des bassins versants. In : Cahiers techniques de la FAO : 1-11.

Renard, KG., Foster, GR., Weesies, GA., Porter, JP., 1991. RUSLE: revised universal soil loss equation. J Soil Water Conserv, 46(1): 30–33

Ricci, GF., De Girolamo, AM., Abdelwahab, OMM., Gentile, F., 2018. Identifying sediment source areas in a Mediterranean watershed using the SWAT model Land Degrad. Dev., 29: 1233-1248, https://doi.org/10.1002/ldr.2889

Roose, E., 1996. Land husbandry - Components and strategy by Director of Soils Research. InFao Soil Bulletin. 70, p. 380.

Shin, G., 1999., The analysis of soil erosion analysis in watershed using GIS." Department of Civil Engineering, Gang-won National University, Gangwon-do, South Korea, Ph. D. dissertation.

Simonneaux, V., Cheggour, A., Deschamps, C., Mouillot, F., Cerdan, O., Le Bissonnais, Y., 2015. Land use and climate change effects on soil erosion in a semi-arid mountainous watershed (High Atlas, Morocco). Journal of Arid Environments, 122, 64-75. https://doi.org/10.1016/j.jaridenv.2015.06.002

Tarolli, P., Cavalli, R., Masin, R., 2019. High-resolution morphologic characterization of conservation agriculture. Catena, 172 : 846-856, https://doi.org/10.1016/j.catena.2018.08.026

Tan, Z., Leung, LR., Li, HY., Tesfa, T., Zhu, Q., Huang, M., 2020. A substantial role of soil erosion in the land carbon sink and its future changes. Global Change Biol., 26: 2642-2655, https://doi.org/10.1111/gcb.14982

Wischmeier, WH., Smith, DD., 1978. Predicting rainfall erosion losses: a guide to conservation planning, Department of Agriculture, Science and Education Administration.

Yjjou, M., Bouabid, R., El Hmaidi, A., Essahlaoui, A., El Abassi, M., 2014. "Modélisation de l'érosion hydrique via les SIG et l'équation universelle des pertes en sol au niveau du bassin versant de l'Oum Er-Rbia." The International Journal of Engineering and Sci (IJES) 3(8), 83-91.

Zingg, AW., 1940. Degree and length of land slope as it affects soil loss in run-off. Agric. Engng. 21: 59-64.

Zouagui, A., Sabir, M., Naimi, M., Chikhaoui, M., Benmansour, M., 2018. Modelisation du risque d'érosion hydrique par l'équation universelle des pertes en terre dans le Rif occidental : cas du bassin versant de Moulay Bouchta (Maroc). European Sci Journal 14(3), 1857-1788.